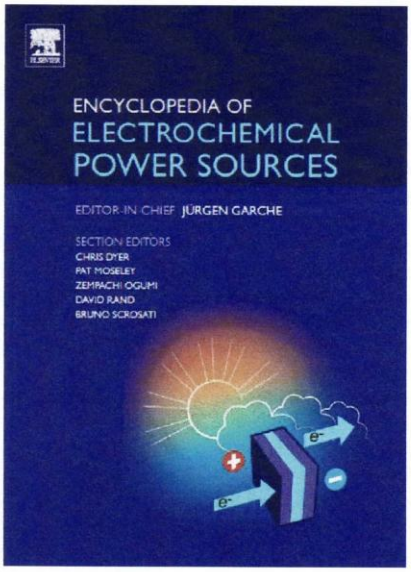

Ugo P, Moretto LM, Scrosati B. Nanoelectrodes. In: Juergen Garche, Chris Dyer, Patrick Moseley, Zempachi Ogumi, David Rand and Bruno Scrosati, editors. Encyclopedia of Electrochemical Power Sources, Vol 2. Amsterdam: Elsevier; 2009. pp. 92–102.

Nanoelectrodes

P Ugo and LM Moretto, University Cà Foscari of Venice, Venice, Italy
B Scrosati, University La Sapienza, Rome, Italy

Introduction

Nanoelectrode ensembles (NEEs) are nanotech-based electroanalytical tools that find application in a variety of fields ranging from electroanalysis to sensors and electronics. The NEEs are fabricated by growing metal nanowires in the pores of a template microporous membrane. The density of the pores in the template determines the number of nanoelectrode elements per surface unit and the average distance between the nanoelectrode elements. The preparation of nanoelectrode using microporous membranes as templates distinguishes itself for its simplicity and wide applicability. A scheme of the membrane template procedure is shown in Figure 1.

Historically, fundamentals of template synthesis in microporous membranes were introduced by G. E. Possin and refined by W. D. Williams and N. Giordano, until the technique was brought to new life at the end of 1980s in Charles Martin's laboratory, shortly followed by others, who proposed the use of preformed microporous membranes to build specially featured electrodes inside the pores of the membrane. The thickness of the template membrane is usually much larger than the pore diameter; therefore, the obtained nanostructures are characterized by high aspect ratio (that is the length/diameter ratio), which can be as high as 600 or more.

The use of preformed microporous membranes as template for the synthesis of nanomaterials was somehow revolutionary because it made accessible to almost any laboratory a simple but effective procedure for the easy preparation of nanomaterials of interest not only to the electrochemist, but to all material scientists. What is needed for the membrane-based synthesis of nanomaterials is a very simple apparatus, such as apparatus for metal deposition and basic electrochemical instrumentation. Characterization is performed electrochemically, spectrophotometrically, by optical, scanning electron, or scanning probe microscopies.

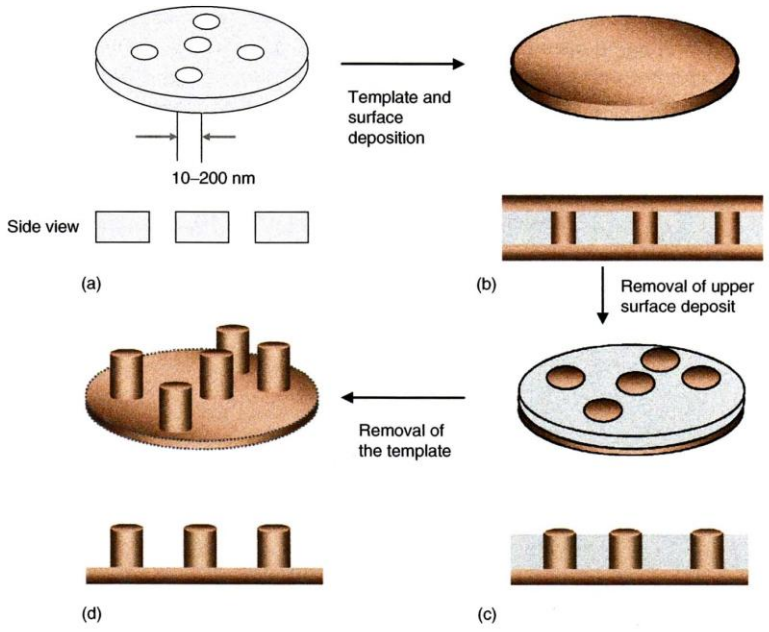

Figure 1 Schematic representation of the procedure used for metal deposition in template membranes. (a) Template with nanometer-sized pores; (b) membrane after metal deposition inside the pores and on the outer faces; (c) ensemble of nanodiks electrodes obtained after cleaning one face two-dimensional nanoelectrode ensemble (2D-NEE); (d) ensemble of nanowire electrodes obtained after etching the template three-dimensional nanoelectrode ensemble (3D.NEE).

Template membranes can be used to produce nanostructured electrode system not only via template metal deposition, but also using other methods such as sol–gel or chemical vapor deposition.

Template Electrochemical Deposition

The two types of template membranes most commonly used for nanoelectrode preparation are (1) microporous alumina and (2) track-etched polymer membranes. Both kinds of membranes are commercially available from suitable producers; note that alumina membranes can also be prepared at a laboratory scale using suitable electrochemical apparatus. Details on the methods for the preparation and characteristics of both kinds of membranes have been reviewed recently by P. Ugo and L. M. Moretto.

For the present goals, it is worth stressing the main differences between alumina and track-etched polymer membranes. Alumina membranes, which are prepared by controlled anodization of aluminum, are characterized by very high pore densities so that the ratio between the pore area and the overall geometric area is a number not much smaller than unity (see **Figure 2(a)**). On the contrary, as shown in **Figure 2(b)**, track-etched polymeric membranes are characterized by much smaller pore densities. They are prepared by irradiation of the polymer foil with nuclear fission fragments of heavy elements such as californium or uranium or by ion beams from accelerators. The tracked zone is then removed by a chemical etching agent, typically a solution of a strong alkali. The chemical etching determines the pore size and shape, whereas the time of tracking determines the pore density. Polymeric materials most widely used for preparing track-etched porous membranes are polycarbonate, polyethylene terephthalate, and polyimide.

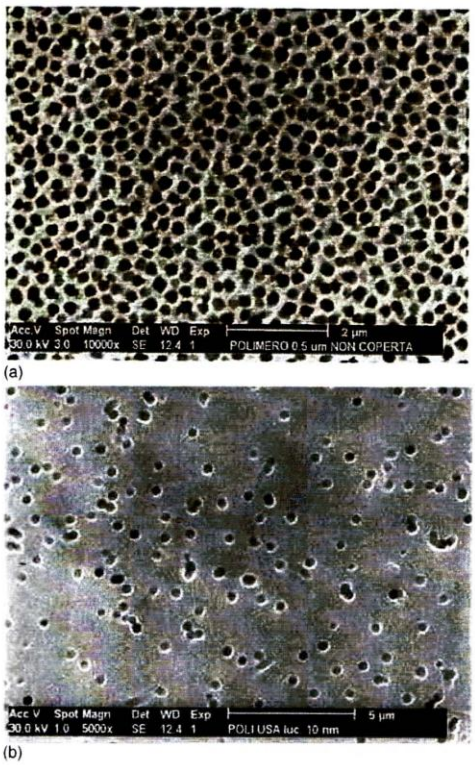

Figure 2 Scanning electron microscopy (SEM) images of commercial microporous membrane with pores of 200 nm diameter: (a) alumina; (b) track-etched polycarbonate.

Advantageous characteristics of the track-etched membranes over porous alumina films are their flexibility (alumina films are brittle) and their smooth surfaces. A problem with track-etched membranes is that the pores created by fission fragment tracks are not always parallel to each other and are randomly distributed, unless special control procedures are applied. On the contrary, the pores in the alumina membranes can be branched on one side of the membrane. Both kinds of membranes can be used for preparing NEEs; track-etched polymers are preferred when high distances between the nanoelectrode elements are required (as in the case of analytical/sensing applications), whereas alumina membranes are the template of choice when high-density nanostructures represent the final goal (as in the case of high-surface nanostructures for battery purposes). Alumina membranes are resistant to organic solvents whereas polymer membranes (in particular, polycarbonate membranes) can be dissolved; however, the former can be damaged or dissolved by alkaline or acidic aqueous solutions.

Template Electrochemical Deposition

Electrochemical deposition of metals in template membranes requires that one side of the membrane be in direct contact with a metallic layer. This can be produced by plasma or vacuum deposition of a metal layer on one side of the membrane, or by tightly attaching the membrane on the surface of a solid electrode. The metal that produces the conductive layer can be the same or different from the one that will provide the final template structure.

The deposition can be carried out under galvanostatic or potentiostatic conditions. The scheme for the cell assembly used for galvanostatic template synthesis is shown in **Figure 3**. For performing the template deposition, the metal-coated template is placed in an electrochemical cell where it acts as the cathode. The electrochemical process consists of the progressive growth and filling of the pores, starting from the bottom

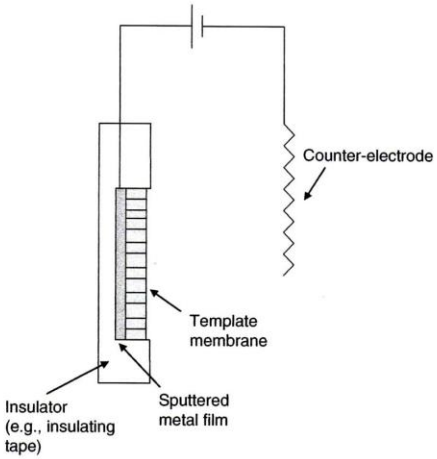

Figure 3 Schematic representation of the electrode system used for galvanostatic template deposition.

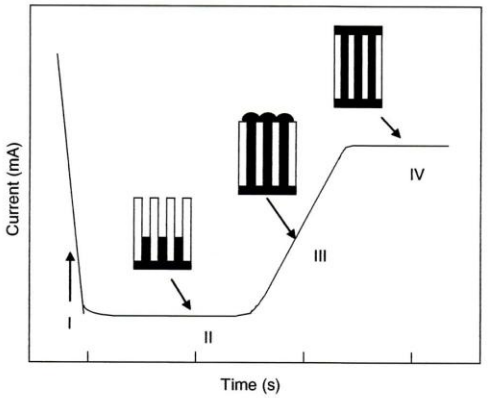

Figure 4 Dependence of the electrochemical reduction current on time for the potentiostatic deposition of a metal in a microporous membrane. Region I: double-layer charging; region II: growth of metal wires inside the pores; region III: start of the growth on the outer surface; region IV: complete coating and growth of the outer deposit.

metallic layer and progressing toward the open end of the template pore (see **Figure 4**).

In a potentiostatic electrochemical deposition, in a microporous template, different distinct regions characterize the time evolution of the current. With reference to the typical behavior shown in **Figure 4**, region I defines the double-layer charging process, in region II metal wires grow inside the pores, in region III the pores are completely filled and the growth starts on the outer face, and in region IV the outer face of the membrane is completely coated by the deposit.

Electrodeposition of metals has been studied for obtaining metal nanowires in alumina, mica, and polycarbonate microporous templates. One problem encountered in electrochemical deposition of metals in polycarbonate template is related to the low wettability of this polymer, which can be improved by impregnation with polyvinylpyrrolidone or by adding 1–2% gelatin to the electrodeposition baths.

Electroless Deposition

Since template membranes are made of insulating material, the possibility to exploit chemical deposition methods such as electroless deposition should be considered. Such process involves the use of chemical reducing agents to plate a metal from a solution onto a surface. The key requirement is to arrange the chemistry so that the kinetics of homogeneous electron transfer from the reducing agent to the metal ion is very slow. A catalyst that accelerates the rate of metal ion reduction is applied to the surface that is to be coated. As a consequence, the metal ion is reduced preferentially at the surface incorporating the catalyst so that only this surface is coated with the desired metal. The thickness of the metal film deposited can be controlled by varying the plating time.

The principles of electroless deposition in microporous membranes are exemplified for the typical case of Au template deposition, as developed by V. P. Menon and C. R. Martin: (1) application of a 'sensitizer' (Sn^{2+}) to surfaces (pore walls plus faces) of the template membrane; (2) activation by immersion into an aqueous silver–ammonia solution; elemental silver is deposited by reaction with Sn^{2+}; (3) formation of gold nuclei by galvanic displacement of silver particles by immersion of the activated membrane in an electroless gold plating bath; and (4) addition of a reducing agent, typically formaldehyde; the gold nanoparticles previously deposited catalyze the further deposition of gold on the pore walls and the membrane surfaces.

In order to slow down the kinetics of the deposition and filling of the pores completely, the process is performed at about 0 °C. The gold electroless plating bath can be a commercial solution containing sodium gold sulfite ($NaAu(SO_3)_2$), or home-made electroless plating baths.

In the electroless method, the growth of the metal layer starts from the sensitized/activated sites located on the pore walls, so that the deposition progresses from the pore walls to the center. This is the reason why, by stopping the deposition within a short time, hollow metal nanomaterials (e.g., nanotubes) can also be prepared. For the nanotube formation, the control of the electroless bath at pH ≈ 10 was proposed. For the preparation of NEEs, metal nanowires are formed by continuing the deposition for 24 h. Typically, the nanowires are kept

inside the guest membrane through a solid sealing with the polymer membrane. This is obtained by shrinking of the polymer by heating above its glass transition temperature (150 °C for polycarbonate). Also, other metals such as copper, palladium, and nickel–phosphorus can be deposited in polycarbonate templates by suitable electroless deposition procedures.

Nanoelectrode Ensembles

Depending on the final surface morphology of the NEE, one can prepare two-dimensional nanoelectrode ensembles (2 D-NEEs) as those shown in **Figure 1(c)**, made of ensembles of nanodisk electrodes, or three-dimensional nanoelectrode ensembles (3 D-NEEs), made of nanofibers as schematized in **Figure 1(d)**. The typical assembly used to transform a piece of golden membrane into a handy device incorporating a 2 D-NEE is shown in **Figure 5**. At the present status of research, in NEEs, all the nanoelectrodes are connected to each other by a back metal current collector, so that all the nanoelectrodes experience the same applied potential. Theoretical treatment of the electrochemical behavior of NEEs was developed systematically only for the nanodisk case (2 D-NEE), as will be presented in the following section; however, some recent results concerning the characterization of the electrochemical behavior of 3 D-NEEs will also be discussed.

Diffusion at Ensembles of Nanodisk Electrodes

The electrochemical characteristics that distinguish 2 D-NEEs from conventional electrodes are

- dramatic lowering of double-layer charging (capacitive) currents;
- extreme sensitivity to the kinetics of the charge transfer process, which means capability to measure very high charge transfer rate constants.

The 2 D-NEE can be considered as ensembles of disk ultramicroelectrodes separated by an electrical insulator interposed between them. At such small electrodes, edge effects from the electrode become relevant and diffusion from the bulk solution to the electrode surface is described in terms of radial geometry instead of the simpler linear geometry used for larger (>100 μm) electrodes. Since in templated NEEs the number of nanodisk elements/surface is large (10^6–10^8 elements cm^{-2}), all the nanoelectrodes are statistically equivalent and the different contribution of the elements at the outer range of the ensemble can be considered negligible even in NEEs of overall area as small as 10^{-2}–10^{-3} cm^2.

The 2 D-NEEs can exhibit three distinct voltammetric response regimes depending on the scan rate or distance between the nanoelectrode elements. When diffusion hemispheres are shorter than average hemidistance between electrodes (high scan rates), the current response is dominated by radial diffusion at each single element (pure radial conditions in **Figure 6(a)**).When radial diffusion boundary layers overlap totally (radius of diffusion hemisphere larger than average hemidistance between electrodes, slow scan rates), 2 D-NEEs behave as planar macroelectrodes with respect to faradaic currents (total overlap conditions), but not for capacitive background currents (see section 'Faradaic-to-Capacitive Current Ratios'). At very high scan rates, the linear active state is reached in which the current response is governed by linear diffusion to the individual nanodisk (linear active conditions, not shown). The diffusion regime usually observed at 2 D-NEEs prepared from commercial track-etched membranes is the total overlap regime.

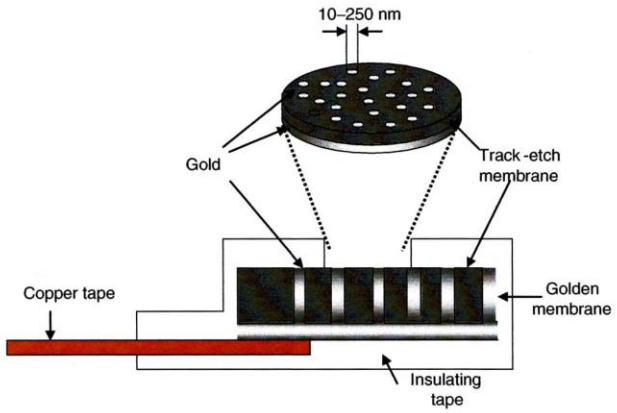

Figure 5 Schematic diagram (section) of the typical assembly of a nanoelectrode ensemble (NEE).

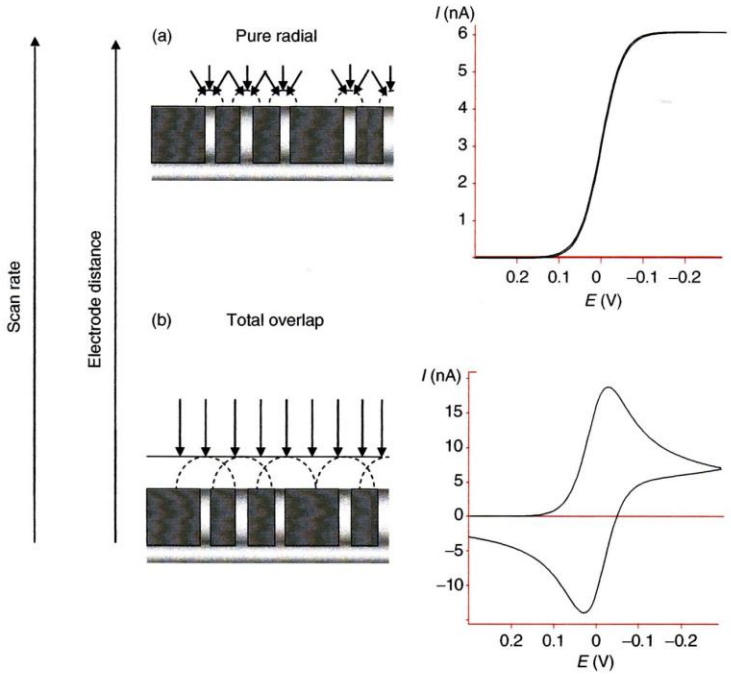

Figure 6 Typical diffusive regimes observed at nanoelectrode ensembles (NEEs) as a function of the scan rate and/or nanoelectrodes distance: (a) pure radial condition; (b) total overlap condition.

Faradaic-to-Capacitive Current Ratios

Under total overlap diffusion regime, 2 D-NEEs show enhanced electroanalytical detection limits, relative to a conventional millimeter-sized electrode. This is because the faradaic current (I_F) at the NEE is proportional to the total geometric area (A_{geom}, nanodisks plus insulator area) of the ensemble, whereas the double-layer charging or capacitive current (I_C) is proportional only to the area of the electrode elements (active area, A_{act}). In voltammetry, I_F is the signal whereas I_C is the main component of the noise. Faradaic-to-capacitive currents at 2 D-NEEs and conventional electrodes with the same geometric area are related by eqn [1]:

$$\left(\frac{I_F}{I_C}\right)_{NEE} = \left(\frac{I_F}{I_C}\right)_{conv} \frac{A_{geom}}{A_{act}} = \left(\frac{I_F}{I_C}\right)_{conv} \frac{1}{f} \qquad [1]$$

where f is the fractional area defined as follows:

$$f = \frac{A_{act}}{A_{geom}} \qquad [2]$$

Typical f values for 2 D-NEEs are between 10^{-3} and 10^{-2}. As shown in **Figure 7**, faradaic currents at 2 D-NEEs are equal to those recorded at macroelectrodes of the same geometric area; however, at 2 D-NEEs capacitive background currents are dramatically lowered. Such an improvement in the faradaic-to-capacitive currents ratio explains why detection limits at 2 D-NEEs can be 2–3 orders of magnitude lower than with conventional electrodes.

It was shown that 2 D-NEEs can be advantageously used not only as naked nanoelectrode ensembles, but also as polymer-coated devices. For instance, the overall surface of an NEE (insulator and nanodisks) can be easily coated by a thin layer of an ion-exchange (ionomer) coating. Such an approach allows the successfull combination of the preconcentration capabilities of ionomer-coated electrodes with the increased faradaic/capacitive current ratio typical of 2 D-NEEs.

As shown by P. Ugo and coworkers, the ability of 2 D-NEEs to furnish well-resolved cyclic voltammograms for trace redox species has interesting consequences also for adsorption-related problems, as in the case of small organic redox molecules and some biomacromolecules as well.

Electron Transfer Kinetics

An important characteristic of NEEs, both 2 D-NEEs and 3 D-NEEs, is that electron transfer kinetics appears

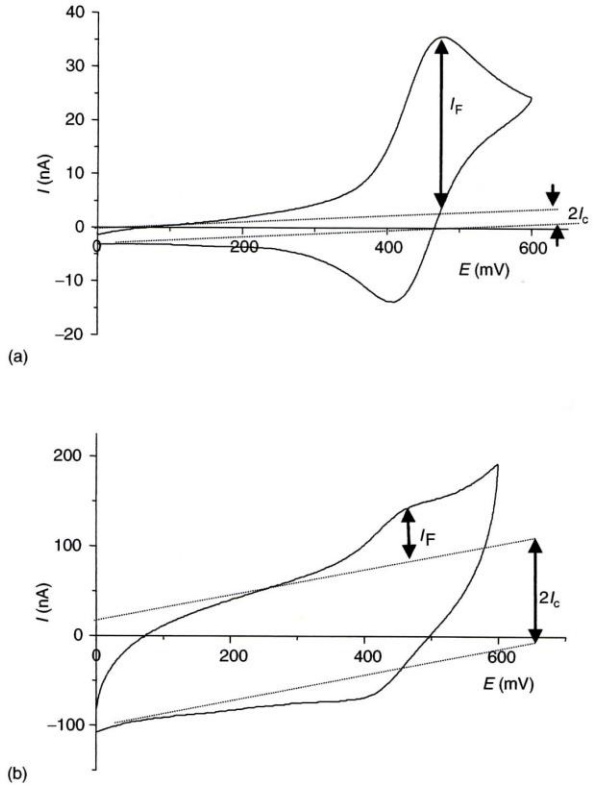

Figure 7 Cyclic voltammograms recorded in 10^{-3} mol L^{-1} $NaNO_3$ supporting electrolyte solution containing 5×10^{-6} mol L^{-1} ferrocenylmethyltrimethyl ammonium cation as reversible redox probe: (a) at nanoelectrode ensemble (NEE); (b) at a Au-disk electrode (for both measurements: scan rate 20 mV s^{-1} and $A_{geom} = 0.07\,cm^2$). I_F is the faradaic peak current (analytical signal) and I_C is the double-layer charging current (background signal). Reproduced from Ugo P and Moretto LM (2006) Template deposition of metals. In: Zoski C (ed.) *Handbook of Electrochemistry*, Section 16.2, pp. 678–709. Amsterdam: Elsevier.

slower than at single electrodes. Being composed of a large number of nanodisk metal elements surrounded by a large surface of insulating material (the guest membrane), NEEs can be considered as electrodes with partially blocked surface (PBE). According to the pioneering model elaborated by C. Amatore, the current response at this kind of electrodes is identical to that of a naked electrode of the same overall geometric area, but with a smaller apparent standard rate constant for the electron transfer, which decreases as the coverage with the blocking agent increases. Such an apparent rate constant (k°_{app}) is related, in fact, to the true standard charge transfer rate constant (k°), by the relationship

$$k^\circ_{app} = k^\circ(1 - \vartheta) = k^\circ f \qquad [3]$$

where ϑ is the fraction of blocked electrode surface and f is defined by eqn [2].

From a mechanistic viewpoint, this means that with NEEs it is easier to obtain experimentally very large k° values. What is measured at NEE is the smaller k°_{app}, which can be converted into the larger k° by eqn [3].

Preparation and Characterization of Three-Dimensional Nanoelectrode Ensembles

S. Yu and coworkers first proposed the controlled removal of polycarbonate from an NEE by using oxygen plasma. This allows one to obtain 3 D-NEEs made of ensembles of metal nanowires. More recently, it was shown that 3 D-NEEs can be obtained from 2 D-NEEs also by chemical etching, using a solvent mixture of dichloromethane and ethanol as the etching agent.

In order to take the maximum advantage from the use of 3 D-NEEs, one has to take into account that their electrochemical response is influenced by the high

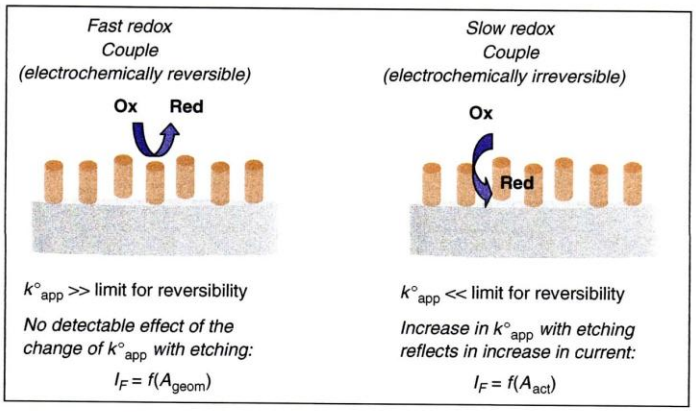

Figure 8 Sketch of the effect of different electron transfer kinetics on electrochemical responses at three-dimensional nanoelectrode ensemble (3 D-NEE).

density of metal nanofibers ($\sim 6 \times 10^8$ nanofibers cm^{-2}), and overlap of the diffusion layers.

In a detailed study on the factors influencing the electrochemical behavior of 3 D-NEEs, M. De Leo and coworkers demonstrated that, for fast redox couples such as ferrocene derivatives, faradaic peak currents are practically uninfluenced by the etching process, while double-layer capacitive currents are influenced. This is explained taking into account that the redox species studied undergoes a fast electron transfer process. Since 3 D-NEEs behave as PBE, the true kinetic constant is substituted by an 'apparent kinetic constant' given by eqn [3]. However, for a very fast redox couple, the influence of the change of $k°_{app}$ values by changing f cannot be appreciated experimentally at the scan rates typically used for cyclic voltammetry (100 mV s^{-1} or lower). As predicted on the basis of the theoretical model of C. Amatore, the situation changes dramatically for redox species characterized by slow heterogeneous electron transfer kinetics. The kinetic limitation causes a considerable torsion of the lines of flux near each nanoelectrode element, thus imposing a local rate of diffusion considerably larger than the one far from each electrode. Under these conditions, each nanoelectrode behaves like an individual element as far as heterogeneous kinetics is concerned. **Figure 8** reports a sketch summarizing the effect of differences in heterogeneous rate constants on the electrochemical behavior of 3 D-NEEs.

Nanoelectrode Ensembles for Batteries

One applied field that can benefit from the nanostructuring of electrodes is the lithium batteries field. The chemistry of these batteries has not changed since their introduction in the market in the early 1990s. Basically, a lithium-ion battery consists of a lithium-ion intercalation negative electrode (generally graphite) and a lithium-ion intercalation positive electrode (generally the lithium metal oxide, lithium cobalt oxide ($LiCoO_2$), or, occasionally, the lithium manganese spinel $LiMn_2O_4$), these being separated by a lithium-ion conducting electrolyte, e.g., a solution of lithium hexafluoro phosphate ($LiPF_6$) in an ethylene carbonate–diethylcarbonate mixture.

Although lithium-ion batteries are still a commercial success, it is clear that they are reaching the limits in performance by using the current electrode materials. For the new generations of rechargeable lithium batteries, a further step in performance is essential. Nanotechnology is the best tool for achieving this breakthrough; it is in fact expected that passing from bulk to nanostructures, one may (1) favor higher interfacial area, which leads to higher charge/discharge rates; (2) provide short path lengths for Li^+ ion transport, which results in increase in power capabilities; and (3) achieve accommodation of the strain of lithium insertion/removal, which improves cycle life.

Graphite is the most common anode material used in lithium-ion batteries. Graphite has a good cycling stability, but a relatively low specific capacity, i.e., not exceeding 372 mAh g^{-1}. Thus, if an improvement in energy content is desired, new, high-capacity alternative anode materials have to be developed. In this respect, metals and semiconductors that store lithium, such as aluminum, tin, and silicon, are among the best candidates. For instance, the lithium–silicon alloy has, in its fully lithiated composition lithium silicide (Li_4Si), a theoretical specific capacity of 4200 mAh g^{-1}, i.e., a value 1 order of magnitude larger than that of conventional graphite. Other examples are given in **Table 1**.

The accommodation of this large amount of lithium is accompanied by enormous volume changes in the host

Table 1 Theoretical specific capacity for selected lithium storage metals in comparison with graphite and metallic lithium

Unlithiated material	*Fully lithiated material*	*Specific capacity ($mAh\,g^{-1}$)*	*Capacity density ($mAh\,cm^{-3}$)*
Al	LiAl	993	1374
Sn	$Li_{4.4}Sn$	994	2025
Si	Li_4Si	4200	2323
C, graphite	LiC_6	372	760
Metallic lithium	Li	3860	2047

material. These in turn induce severe mechanical strains which lead the electrode to crack and, eventually disintegrate in the round of few cycles. An illustrative example is provided in **Figure 9**, which shows the evolution of the morphology of an aluminum electrode in the course of the initial charge (lithium alloying)–discharge (lithium removal) cycles in a lithium cell.

A way to solve this problem is to modify the morphology of the metal alloy electrodes by reducing their particle size to few nanometers and/or by designing special nanostructures. Indeed, this strategy is expected to have a twofold effect on the performance of the electrodes: (1) improvement in cycling stability, because small particles enable the accommodation of the mechanical strains more easily (the absolute volume changes are smaller than for larger particles, although the relative changes are the same) and (2) enhancement of power owing to the reduction of the lithium-ion diffusion length. The validity of this strategy has been confirmed by various authors.

Undoubtedly, alloy performance can benefit from nanostructures. For instance, thin amorphous silicon films deposited on specially roughened copper foil surface were shown to have close to 100% reversibility at specific capacities exceeding $3000\,mAh\,g^{-1}$. Good capacity retention was also found for silicon electrodes prepared with a nanopillar surface morphology (see scanning electron microscope (SEM) image in **Figure 10**). In this case, the stability of the electrode was obtained by size confinement, which alters particle deformation and reduces fracturing.

Nanostructures are also highly beneficial for other classes of electrode materials, e.g., for metal oxides. For instance, it is known that tin oxide can electrochemically react with lithium with a first process involving the formation of lithium oxide and tin, followed by a lithium–tin alloying–dealloying reversible process. It is assumed that the 'in situ' formed lithium oxide can act as a 'buffer' for accommodating the volume changes that accompany the second alloying process. However, if common electrode morphologies are used, the cycling stability of the tin oxide electrode is still unsatisfactory.

Also in this case, considerable improvements are obtained moving to nanostructures. **Figure 11** shows the

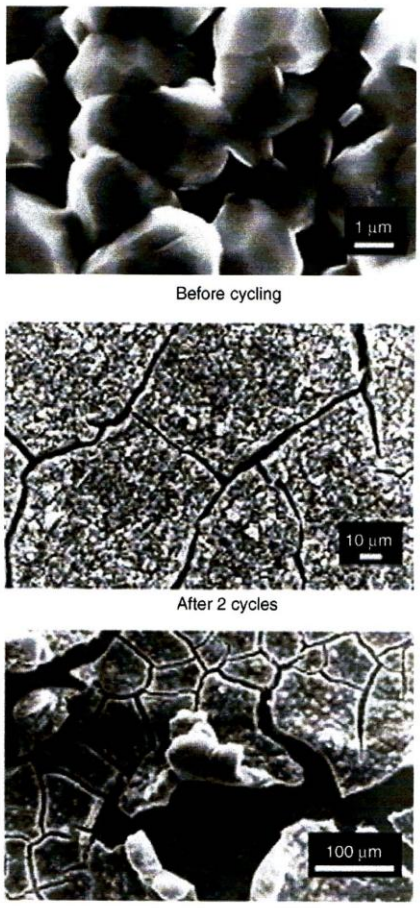

Figure 9 Changes in the morphology of a tin electrode after charge (lithium alloying)–discharge (lithium removal) cycles in a lithium cell. The mechanical strain generated during the cycles leads to cracking of the electrode with resulting marked loss of capacity in the course of a few cycles. Reproduced from Winter M and Besenhard JO (1999) Electrochemical lithiation of tin and tin-based intermetallics and composites. *Electrochimica Acta* 45: 31–50.

morphology of tin oxide prepared in the form of nanowires using the template technique. The electrode material is deposited within the pores of the membrane by a solution-based method. For instance, in the case of the tin oxide (SnO_2) preparation, the membrane was immersed in a solution of tin chloride ($SnCl_2$), hydrogen chloride, and ethyl alcohol and then applied to the surface of a platinum current collector. The membrane is then removed by burning it in oxygen plasma. This leaves nanofibers of the desired electrode materials, which in the case of tin oxide were 110 nm in diameter and 6.0 mm in length.

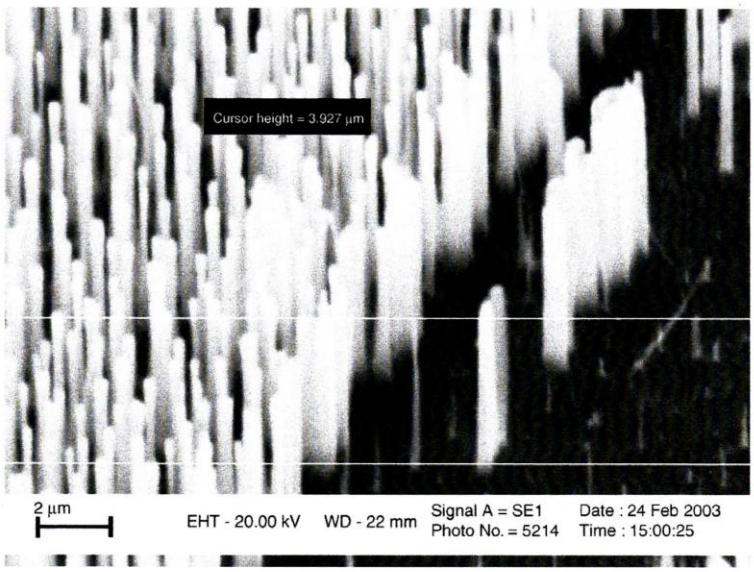

Figure 10 Scanning electron microscopy (SEM) image of a silicon electrode having a nanopillar surface morphology. This morphology provides free volume configurations, which are able to accommodate the massive volume changes occasioned by lithium alloying/dealloying. Courtesy of Professor M. Green from Imperial College, London.

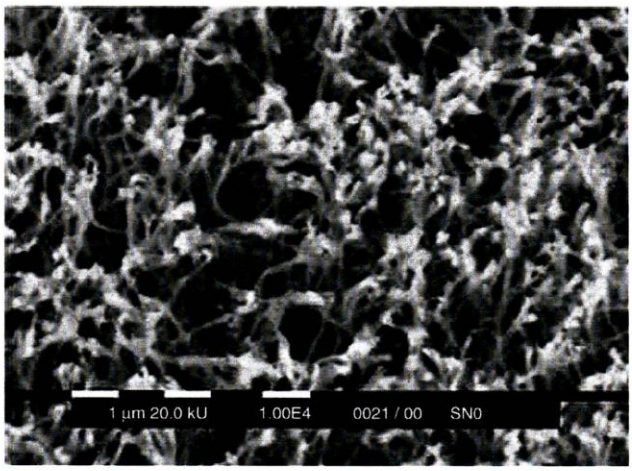

Figure 11 Scanning electron microscopy SEM image of a tin oxide electrode having a nanofibril morphology. The structure consists of nanodisperse 110 nm SnO_2 fibers protruding from a current collector surface like the bristles of a brush. Reproduced from Li N, Martin CR, and Scrosati B (2001) Nanomaterial-based Li-ion battery electrodes. *Journal of Power Sources* 97–98: 240–243.

This procedure gives unique electrode structures having dramatically improved rate and cycling performance associated with the small size of the nanofibers and the small domain size of the metal alloy grain within the nanofibers. For instance, tests in a lithium cell have demonstrated that the nanofiber SnO_2 electrode is able to operate at rates as high as $8\,C$ with a stable specific capacity of the order of $700\,\mathrm{mAh\,g^{-1}}$, values never achieved with conventional electrode structures, such as graphite.

Also, critical for the progress of lithium batteries are improvements at the cathode side. For instance, the

replacement of the high cost, partially toxic lithium cobalt oxide with more affordable and sustainable materials, would be highly welcomed. The nanotechnology approach is here much less developed than in the case of the anodes. In fact the use of nanoparticulate forms of the classical cathode materials such as lithium cobalt oxide can lead to significant reaction with the electrolyte, and ultimately, safety problems, especially at high temperatures, compared with the use of materials in the micron range. Therefore, the nano approach may be safely adopted for those electrode materials having voltage profiles falling within the stability window of the electrolyte. In these cases, the many advantages of nanoparticles may be exploited more easily. An example is the phospho-olivine lithium ferrous phosphate ($LiFePO_4$) that, in a lithium cell, may be reversibly delithiated to ferrous phosphate ($FePO_4$) with an operating voltage averaging around 3.5 V versus lithium, i.e., a value largely within the stability window of the most common lithium-ion electrolytes. Indeed, $LiFePO_4$ is an appealing cathode for lithium batteries: it is cheap, environmentally benign, and has a reasonably high specific capacity, i.e., approaching that of lithium cobalt oxide ($170\,mAh\,g^{-1}$ versus $220\,mAh\,g^{-1}$).

However, the kinetics of this electrode is controlled by its poor electronic conductivity and by the low lithium-ion diffusion across the reaction phases. Morphological modification at the nano scale level appears to be the proper tool to control these undesired phenomena. Recent literature has shown that strategies such as carbon nanopainting, nanofibril textures, and carbon nanodispersion led to excellent improvements in the utilization of the 'per se' insulating lithium ferrous phosphate.

Another strategy for enhancing the performance of lithium ferrous phosphate electrodes is preparing them in a nanofibril structures. A sol–gel method was used to deposit the lithium ferrous phosphate nanofibers within the pores of the template membrane. Contrary to the usual procedure where the template is totally removed to yield nanofibers protruding from an underlying current collector surface, in this case, the polycarbonate membrane was pyrolyzed in a reducing environment in order to yield graphitic carbon particles intimately mixed with the lithium ferrous phosphate nanofibers, to finally obtain a nanocomposite $LiFePO_4$/carbon matrix.

This $LiFePO_4$/carbon nanocomposite electrode structure is suited for high-rate applications because the distance that Li^+ must diffuse in the electrode is limited by the radius of the nanofibers and because the carbon matrix provides for good electronic contact through the composite. Indeed, electrochemical tests in lithium cells have confirmed that these nanocomposite electrodes can deliver a specific capacity of $150\,mAh\,g^{-1}$ at a rate of 5 *C* and maintain a substantial fraction of the theoretical capacity even at rates exceeding 50*C*.

Clearly, there are pros and cons in any new approach. However, the results quoted here show that moving from traditional bulk structures to nanostructures can significantly change the properties of electrode–electrolyte interfaces and consequently their performance in electrochemical devices, this being particularly valid for the case of lithium batteries. Although some risk may be associated to the high surface area of nanostructured electrode materials, nanotechnology is the right tool for yielding quantum jumps in battery performance.

Concluding Remarks

The template synthesis makes the preparation of electrode systems with critical dimensions in the domain of nanometer accessible to almost any electrochemical laboratory. The use of microporous templates constitutes indeed an attractive and practical methodology for the preparation of a variety of nanomaterials characterized by high aspect ratio, such as nanowires and nanotubes of metals, metal oxides, salts, conducting polymers, and composites. These nanomaterials show peculiar and advantageous performances for many electrochemical applications, which span from electroanalysis to energy storage.

For electroanalytical and sensing applications NEEs show dramatically enhanced signal-to-background ratios with respect to any other electrode system, together with the possibility to measure rather easily very fast charge transfer kinetic constant of interest for fundamental studies.

The development of templated nanostructured electrodes for batteries applications assists in overcoming some of the limits of conventional electrochemical energy storage systems, in particular, as far as improvements in the cyclability of the electrode materials is concerned. In the immediate future it is reasonable to think that NEEs can contribute to the development of highly miniaturized electrochemical systems for sensing purposes and energetics, both topics being very interesting for advanced and frontier applications.

Nomenclature

Symbols and Units

A_{act}	active area
A_{geom}	geometric area
f	fractional electrode area
I_C	capacitive current
I_F	faradaic current
k^o	heterogeneous electron transfer rate constant
k^o_{app}	apparent rate constant

ϑ	fraction of the blocked electrode surface
Abbreviations and Acronyms	
2D-NEE	two-dimensional nanoelectrode ensemble
3D-NEE	three-dimensional nanoelectrode ensemble
NEE	nanoelectrode ensemble
PBE	electrodes with partially blocked surface
SEM	scanning electron microscopy

See also: **Electrochemical Theory:** Double Layer; Kinetics; **Materials:** Nanofibers; **Measurement Methods:** Electrochemical: Linear Sweep and Cyclic Voltammetry; **Secondary Batteries – Lithium Rechargeable Systems:** Negative Electrodes: Lithium Metal; **Secondary Batteries – Lithium Rechargeable Systems – Lithium-Ion:** Lithium-Ion Polymer Batteries; Overview.

Further Reading

Amatore C (1995) Electrochemistry at ultramicroelectrodes. In: Rubinstein I (ed.) *Physical Electrochemistry*, pp. 131–208. New York: Marcel Dekker.

Amatore C, Saveant JM, and Tessier D (1983) Charge transfer at partially blocked surfaces. A model for the case of microscopic active and inactive sites. *Journal of Electroanalytical Chemistry* 147: 39–51.

Apel P (2001) Track etching technique in membrane technology. *Radiation Measurements* 34: 559–566.

Aricò AS, Bruce P, Scrosati B, Tarascon J-M, and Van Schalkwijk W (2005) Nanostructured materials for advanced energy conversion and storage devices. *Nature Materials* 4: 366–377.

Bard AJ and Faulkner L (2000) *Electrochemical Methods*, 2nd edn. New York: Wiley.

Croce F, Panero S, Scrosati B, and Wachtler M (2004) Nanotechnology for the progress of lithium batteries R&D. *Journal of Power Sources* 129: 90–95.

De Leo M, Kuhn A, and Ugo P (2007) 3D-ensembles of gold nanowires: Preparation, characterization and electroanalytical peculiarities. *Electroanalysis* 19: 227–236.

Despic A and Parkhutik VP (1989) Electrochemistry of aluminium in aqueous solutions and physics of its anodic oxide. In: Bockris JO'M, White RE, and Conway BE (eds.) *Modern Aspects of Electrochemistry*, vol. 20, pp. 401–503. New York: Plenum Press.

Diggle JW, Downie TC, and Goulding CW (1969) Anodic oxide films on aluminum. *Chemical Reviews* 69: 365–405.

Foss CA (2002) Electrochemical template synthesis of nanoscopic metal particles. In: Feldheim DL and Foss JCA (eds.) *Metal Nanoparticles, Synthesis, Characterization and Applications*, pp. 119–139. New York: Marcel Dekker.

Green M, Fielder E, Scrosati B, Wachtler M, and Serra Moreno J (2003) Structured silicon anodes for lithium battery applications. *Electrochemical and Solid-State Letters* 6: A75–A79.

Hulteen JC and Martin CR (1997) A general template-based method for the preparation of nanomaterials. *Journal of Materials Chemistry* 7: 1075–1087.

Li N, Martin CR, and Scrosati B (2001) Nanomaterial-based Li-ion battery electrodes. *Journal of Power Sources* 97–98: 240–243.

Martin CR (1994) Nanomaterials: A membrane-based synthetic approach. *Science* 266: 1961–1966.

Martin CR and Mitchell DT (1999) Template-synthetized nanomaterials in electrochemistry. In: Bard AJ and Rubinstein I (eds.) *Electroanalytical Chemistry, A Series of Advances*, vol. 21, pp. 1–74. New York: Marcel Dekker.

Menon VP and Martin CR (1995) Fabrication and evaluation of nanoelectrode ensembles. *Analytical Chemistry* 67: 1920–1928.

Nazri G-A and Pistoia G (eds.) (2004) *Lithium Batteries Science and Technology*. Boston: Kluwer Academic Publisher.

Penner RM and Martin CR (1987) Preparation and electrochemical characterization of ultramicroelectrode ensembles. *Analytical Chemistry* 59: 2625–2630.

Possin GE (1970) A method for forming very small diameter wires. *Review of Scientific Instruments* 41: 772–774.

Sides CR, Croce F, Young VY, Martin CR, and Scrosati B (2005) A high-rate, nanocomposite $LiFePO_4$/carbon cathode. *Electrochemical and Solid-State Letters* 8: A484–A487.

Ugo P (2006) Polymer based voltammetric sensors. In: Grimes CA, Dickey EC, and Pishko MV (eds.) *Encyclopedia of Sensors*, vol. 8, pp. 67–85. Stevenson Ranch: American Scientific Publishers.

Ugo P and Moretto LM (2006) Template deposition of metals. In: Zoski C (ed.) *Handbook of Electrochemistry*, Section 16.2, pp. 678–709. Amsterdam: Elsevier.

Ugo P, Moretto LM, Bellomi S, Menon VP, and Martin CR (1996) Ion-exchange voltammetry at polymer film-coated nanoelectrode ensembles. *Analytical Chemistry* 68: 4160–4165.

Ugo P, Moretto LM, and Vezzà F (2002) Ionomer-coated electrodes and nanoelectrode ensembles as electrochemical environmental sensors: Recent advances and prospects. *ChemPhysChem* 3: 917–925.

Ugo P, Pepe N, Moretto LM, and Battagliarin M (2003) Direct voltammetry of cytochrome *c* at trace concentrations with nanoelectrode ensembles. *Journal of Electroanalytical Chemistry* 560: 51–58.

van Schalkwijk W and Scrosati B (eds.) (2002) *Advances in Lithium-Ion Batteries*. New York: Kluwer Academic/Plenum Publishers.

Williams WD and Giordano N (1984) Fabrication of 80 Å metal wires. *Review of Scientific Instruments* 55: 410–412.

Winter M and Besenhard JO (1999) Electrochemical lithiation of tin and tin-based intermetallics and composites. *Electrochimica Acta* 45: 31–50.

Yu S, Li N, Wharton J, and Martin CR (2003) Nano wheat fields prepared by plasma-etching gold nanowires-containing membranes. *Nano Letters* 3: 815–818.